NSRRC - J0 4916 (2015)

Biomacromolecules

Article

pubs.acs.org/Biomac

Zooming in: Structural Investigations of Rheologically Characterized Hydrogen-Bonded Low-Methoxyl Pectin Networks

Bradley W. Mansel,[†,‡] Che-Yi Chu,[§,⊥] Andrew Leis,[¶] Yacine Hemar,[∥] Hsin-Lung Chen,[§] Leif Lundin,[#,▽] and Martin A. K. Williams*[,†,‡]

[†]Institute of Fundamental Sciences, Massey University, Palmerston North 4474, New Zealand

[‡]The Macdiarmid Institute for Advanced Materials and Nanotechnology, Wellington 6140, New Zealand

[§]National Tsing-Hua University, Hsin-Chu 30013, Taiwan

[⊥]National Synchrotron Radiation Research Centre, Hsin-Chu 30076, Taiwan

[¶]CSIRO, Australian Animal Health Laboratory, Geelong 3220, Australia

[∥]The University of Auckland, Auckland 1010, New Zealand

[#]CSIRO Food and Nutrition, Werribee 3030, Australia

Supporting Information

ABSTRACT: Self-assembled hydrogen-bonded networks of the polysaccharide pectin, a mechanically functional component of plant cell walls, have been of recent interest as biomimetic exemplars of physical gels, and the microrheological and strain-stiffening behaviors have been previously investigated. Despite this detailed rheological characterization of preformed gels, little is known about the fundamental arrangement of the polymers into cross-linking junction zones, the size of these bonded regions, and the resultant network architecture in these hydrogen-bonded materials, especially in contrast to the plethora of such information available for their well-known calcium-assembled counterparts. In this work, in concert with pertinent rheological measurements, an in-depth structural study of the hydrogen-bond-mediated gelation of pectins is provided. Gels were realized by using glucona-delta-lactone to decrease the pH of solutions of pectic polymers that had a (blockwise) low degree of methylesterification. Small-angle X-ray scattering and transmission electron microscopy were utilized to access structural information on length scales on the order of nanometers to hundreds of nanometers, while complementary mechanical properties were measured predominantly using small amplitude oscillatory shear rheology.

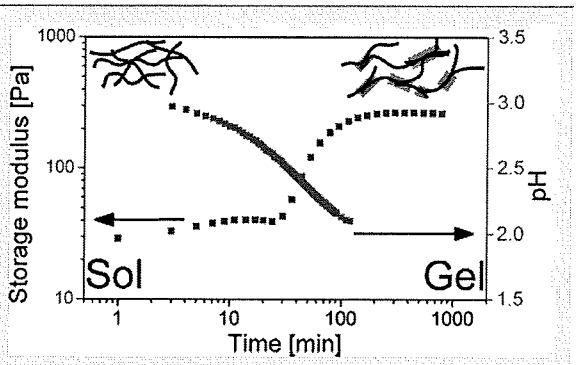

INTRODUCTION

Pectin is a polysaccharide of considerable structural importance in the plant cell wall.[1−4] In tandem with the fundamental biophysical interest in its native mechanical role, there is also significant interest in pectin-based biomaterials from many different industries due to, in-part, its ability to form a solid material with tunable mechanical properties.[5] While divalent-ion-chelating pectin gels have been exploited for many decades, here we report on the structure and mechanical properties of less-exploited hydrogen-bonded pectin gels that can be formed under acidic conditions in the absence of sugar. In the spirit of traditional soft matter physics, we aim to understand the relationship between structure and mechanical properties. Measurements on the structural aspects of such biopolymer materials are typically experimentally challenging in comparison to mechanical measurements, and as such there are considerably fewer structural studies reported in the literature. In particular, there is presently a complete lack of structural data on the acid-induced pectin networks of interest here.

Pectin, as found in the plant cell wall, is a complex heteropolysaccharide consisting of several domains, predominantly homo- and rhamno-galacturonan (RGI and RGII), the disposition of which is still a matter of debate to some extent.[6] It is clear however that the homogalacturonan (HG) backbone is connected through alpha 1−4 linkages and that it is the intermolecular association of this part of the polymer that is primarily responsible for pectin's ion-binding and gel forming capacity.[7] RGI contains rhamnose residues, alternating with those of galacturonic acid, which act as sites of neutral sugar side chain attachment; these branches are often removed during extraction procedures that are used to purify pectin and are

Received: June 29, 2015
Revised: August 19, 2015
Published: August 20, 2015

ACS Publications © 2015 American Chemical Society

DOI: 10.1021/acs.biomac.5b00870
Biomacromolecules 2015, 16, 3209−3216

consequently not usually present in significant amounts in commercially available samples. In the plant cell, pectin is biosynthesised as a weak acid with around 20% of the monomers in each homogalacturanan chain bearing an unesterified carboxyl group, with the remaining groups carrying a methyl ester.[8] The ratio of methyl ester groups to acid groups is referred to as the degree of methyl esterification (DM) and can be modified using chemical or enzymatic procedures. Modifying the degree or pattern of methyl esterification can radically alter the gel forming abilities and mechanical properties of the subsequent gels formed. This makes pectin a particularly attractive biopolymer to design and create soft materials with tailored mechanical properties.

Physical gels are formed through dynamic cross-linking, typically involving ionic interactions, hydrogen bonding, van der Waals interactions, or topological entanglements, and are commonly weaker than gels formed by permanent covalent bonding.[9] Hydrogen bonding between protonated and unprotonated carboxyl groups on neighboring chains has been hypothesized to be involved in the formation of acid-induced low DM pectin gels.[10] To form a stable junction with a binding energy of several kT requires the concerted action of many such bonds, thus explaining the propensity of substrates with very blockwise patterns of demethylesterification and of low DM to form acid gels. While a low DM is required for gel formation, it should be noted that if the degree of methyl esterification is too low, the pectin can precipitate out of solution rather than forming a stable gel. When acid gels do form, they are typically comparatively weak, having storage moduli that rarely exceed hundreds of Pascal.[11,12] This fact, together with the less clear biomimetic relevance of these acid-induced gels, means the majority of research on pectin gels to date has focused on their better known ionotropic networks in which the carboxyl groups chelate divalent metal ions. In this work, pectin is gelled, at ambient temperature, using the hydrolysis and concomitant release of protons from glucono-delta-lactone (GDL) to reduce the solution pH in a controlled manner.

The polyelectrolytic properties, or more precisely the charge density of the pectin polymer, play an important role in determining the physical properties of both its solution and gel states. The linear charge density is a result of the number of unmethylesterified carboxyl groups displayed by the substrate, their distribution along a chain, the protonation state of these groups, and any counterion condensation or screening effects. In general, polyelectrolyte solution behavior can be complex, with much discussion in the literature as to the effects on both the polymer structure and dynamics. The Coulomb interaction is long ranged so that both the intra- and intermolecular interactions of the polymer are expected to be modified by the charge density and distribution. This is exemplified by the conformational change from a 2,1 to 3,1 helix that accompanies the protonation of the carboxyl groups in low DM pectin, which has been detected by circular dichroism and X-ray diffraction.[10] It is thought that the placement of the carboxyl groups induced by this conformational change, facing them out from the polymer backbone, facilitates interchain hydrogen bonding and is key to the acid-induced gelation mechanism.

In the first part of this study, the effects of pH on the structural and viscoelastic properties of a block-wise de-esterified, low DM, pectin solution were explored. Experiments were carried out at pH values both at and below the pK_a over a range that covers the sol–gel transition (between pH 2 and 3 for this particular sample). Small angle oscillatory shear rheology and small-angle X-ray scattering (SAXS) were used to examine the evolution of mechanical and structural properties during the sol–gel transition, and SAXS was further utilized to explore the effects of temperature and solvent on the large-scale structure of the system. For a complete overview of the structure present in an acid-induced pectin gel, transmission electron microscopy (TEM) tomography was carried out on a plastic embedded gel sample, while SAXS experiments were performed on the corresponding unadulterated gel. Small angle scattering techniques provide a unique approach to access the structural properties of soft materials free from freezing or plastic embedding, as is required with real space electron microscopy imaging techniques such as TEM and scanning electron microscopy (SEM), which could significantly perturb the molecular arrangements in these soft systems. The interpretation of the scattering data, which is measured in reciprocal space, can however be challenging compared to real space techniques, and any heterogeneities are preaveraged over the scattering volume during the measurement itself. To completely characterize the structural properties of biopolymer gels, one must not only probe the molecular scale where the individual polysaccharide chains self-assemble, but also probe the microscale where assemblies typically form a large porous network, and correspondingly we performed SAXS using two different instruments to span a larger distance scale and probe large-scale changes in the networks upon heating and cooling.

EXPERIMENTAL SECTION

Polymer and Gel Preparation. The gelation method exploited herein has been described in detail previously.[13] The polymer fine structure modification was performed by first dissolving dried apple pectin (Sigma) in ultrapure water (Milli-Q) to a final polymer concentration of 0.25 wt % and then adjusting the pH to 7 using 1 N and 0.1 N analytical grade sodium hydroxide together with a calibrated digital pH meter. A pH-monitored demethylesterification method was then carried out. The pH of the solution was monitored and held at 7 by slowly adding known volumes of 0.1 N NaOH, to counteract the active pectin methylesterase (PME) enzyme liberating galacturonic acid groups on the polymer backbone from their methyl esters, until the DM was lowered to 40% (as confirmed by capillary electrophoresis). The sample was then heated to 80 °C to denature the PME, frozen using liquid nitrogen, and finally freeze-dried for 24 h to allow for the long-term storage of the dried polymer. Subsequently, a solution was made by dissolving 0.02 g of the freeze-dried pectin in 1.5 mL of deionized water. Next, 0.16 g of GDL was dissolved in 0.32 mL of deionized water and mixed with the pectin solution as quickly as possible to minimize any hydrolysis of GDL occurring before mixing, while being careful not to form bubbles. This solution was then either loaded into the requisite sample cells for SAXS or into the rheometer geometry as described further.

Small-Angle X-ray Scattering. Gel structure was characterized using SAXS experiments that were performed at two different synchrotron facilities. The first experiments were performed at beamline 23A1 at the National Synchrotron Radiation Research Centre (NSRRC) in Hsinchu, Taiwan. Here, samples were held in 2.5 mm path-length cells, sealed with Kapton windows, and irradiated with 15 keV X-rays. A Dextris Pilatus 1 M detector, with a sample-to-detector distance of 3072 mm, collected the scattered radiation. Further information about the beamline optics can be found in ref 14. For heating experiments, acquisitions were made for approximately 1 min, while the sample was moved in the beam to reduce the possibility of radiation damage, and then the sample was heated in 10 °C increments each of 5 min duration, with each heating step followed by 5 min of equilibration time and the acquisition of a further data set.

DOI: 10.1021/acs.biomac.5b00870
Biomacromolecules 2015, 16, 3209–3216

For time-resolved measurements, acquisitions were taken continuously with 10 s exposures for a period of 20 min.

The second round of experiments was performed at the Australian Synchrotron on the SAXS beamline,[15] where samples were prepared in 1.5 mm diameter quartz glass capillary tubes (purchased from Hampton Research or http://capillarytubes.co.uk/) and irradiated with 11 keV radiation. Multiple exposures were averaged over postacquisition to increase the signal-to-noise ratio. For temperature measurements, samples were heated in 5 °C intervals and allowed to equilibrate for 10 min before data were collected between heating steps. Scattered radiation was collected using a Dextrus Pilatus 1 M detector as at NSRRC, although in this case, a longer sample-to-detector distance of 7179 mm was taken advantage of to access information on larger length scales. It should be noted that care was taken to subtract the scattering from GDL using a series of background experiments and that measurements were carried out to ensure radiation damage was not an issue.

Rheology. Rheology experiments were performed using an Anton Paar MCR 302 rheometer equipped with a Peltier-controlled heating plate and a 50 mm cone and plate geometry. All experiments were performed with the gel formed in situ on the rheometer. First time-resolved experiments were performed by imposing a 0.5% strain at 1 Hz to investigate the evolution of the mechanical properties. Once gelation had been fully realized, prestress measurements were performed. An oscillatory shear of between 0.1 and 10 Hz at 0.5% strain was superimposed onto a constant stress, P, which was varied from P = 0.1 to P = 100 Pa to obtain the frequency dependent mechanical properties of the prestressed gel.

Transmission Electron Microscopy. Gels were fixed with 0.1% Ruthenium Red and phosphate buffered 2.5% glutaraldehyde prior to dehydration in a graded ethanol series and embedding in an epoxy resin (ProCure 812, ProSciTech, Thuringowa, Australia). Sections with nominal thicknesses of 150 nm were cut with an ultramicrotome and preirradiated for 15 min at low magnifcation prior to image acquisition. Two-dimensional micrographs and tomographic tilt series were recorded on a JEOL JEM-1400 transmission electron microscope with a LaB6 cathode operated at 120 kV and under low-dose conditions including using a spot size 3 and synchronized beam blanking and acquisition. Projection images were collected on a Gatan Ultrascan 2K × 2K CCD with a pixel size of 0.86 nm (nominal magnification of 12 000×). The tilt increment was 1 degree, and the tilt range was typically ±75 degrees. Tomograms were recorded using "Recorder" software (System in Frontier/JEOL, Japan) and subsequently aligned via fiducial markers using eTomo (NCIM, Boulder, Colorado). The aligned projections were reconstructed using weighted back-projection, again using eTomo.

RESULTS AND DISCUSSION

Structural Analysis of Pectin Solutions. Figure 1 shows the results obtained from SAXS experiments performed on pectin solutions at a range of concentrations made from the premodified, commercially available, apple pectin that was later demethylesterified and subsequently used to form acid gels. Reassuringly, the scattering profiles exhibited by these original pectin solutions are similar to those expected for a semidilute semiflexible polymer solution.[16] It can be clearly seen, particularly as the concentration increases, that the data exhibit two distinct regimes (power law behaviors with exponents of −2.1 and −1 are shown as a guide to the eye). In the low-q (large length-scale) regime, the average fractal dimension of the mesh formed by the overlapping polymer solution can be obtained: −2 would indicate a random arrangement of the polymers in 3D space, and lower fractal dimensions (power law exponents) indicate more expanded arrangements. For the data obtained on these pectin solutions, a slope of approximately −2.1 is obtained, indicating instead that the chains have a moderately clustered conformation and do not fill space as

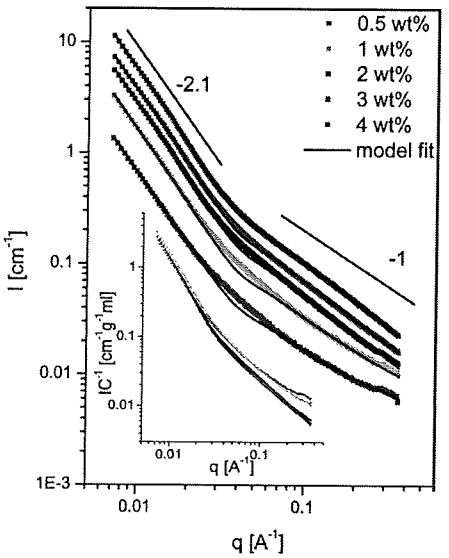

Figure 1. SAXS data recorded from apple pectin solutions as a function of concentration. Fits to the Beaucage model as described in the text are also shown. Two regimes are present: the lower q data corresponding to the arrangement of pectin chains in space and the higher q to the rod-like behavior of a single chain. The inset shows the scattering normalized for concentration.

efficiently as a simple random walk. The high q (short length scale) linear region with a slope of approximately −1 indicates the rod-like nature of the polymers below the persistence length or mesh-size, so that the q-value at which the transition between the regions occurs gives information on the length scale at which the space-filling becomes dominated by the geometrical architecture of the mesh rather than the individual polymers. It should be noted that the relatively long persistence length and small radius of a pectin chain means that the application of many models available for describing polymeric systems would produce redundant parameters, so instead, a generalized power law model in the form of a Beaucage model was fitted to the data (Figure 1, solid lines).

In general, the Beaucage model can be used to describe a system with a Guinier regime describing the average size of the entities comprising the elements of the fractal system, followed by power law regions. Systems such as polymer coils display this type of scattering.[17,18] The modified Beaucage model was used where the intensity as a function of momentum transfer vector, $q = 4\pi/\lambda \sin(\theta/2)$, is described by[18−20]

$$I(q) \cong \left\{ G \exp\left(-\frac{q^2 R_g^{\,2}}{3}\right) + B \exp\left(\frac{-q^2 R_s^{\,2}}{3}\right)\left(\frac{1}{q^*}\right)^p \right\} + \left\{ G_s \exp\left(\frac{-q^2 R_s^{\,2}}{3}\right) + B_s \left(\frac{1}{q_s^*}\right)^{p_s} \right\} \quad (1)$$

where $q^* = q/[\mathrm{erf}(qR_g/6^{0.5})]^3$, $q_s^* = q/[\mathrm{erf}(qR_s/6^{0.5})]^3$, R_s is the radius of gyration of the subunit, G is the Guinier prefactor defined by $G = N_p \Delta\rho^2 V_p^{\,2}$, and $\Delta\rho$ is the change in electronic density, where N_p and V_p are the number of particles and the volume of the particles in the scattering volume, respectively. B and B_s are given below where Γ is the gamma function and p is the power law exponent of the fractal. This model provided by

DOI: 10.1021/acs.biomac.5b00870
Biomacromolecules 2015, 16, 3209−3216

ref 20 and uses the complete expansion of the polymer fractal model:

$$B = \frac{Gp}{R_g^{\,p}}\left[\frac{6p^2}{(2+p)(2+2p)}\right]^{p/2}\Gamma\left(\frac{p}{2}\right) \quad (2)$$

$$B_s = \frac{G_s p_s}{R_s^{\,p_s}}\left[\frac{6p_s^{\,2}}{(2+p_s)(2+2p_s)}\right]^{p_s/2}\Gamma\left(\frac{p_s}{2}\right) \quad (3)$$

For this semiflexible polymer system, the low q scattering is described by the first term in eq 1, and the second term describes the high q scattering. For an entangled polymer system, it is expected that if there are no large scale polymer density fluctuations, the low q regime will span all of space up to the size of the container, and no Guinier regime will be found.

The fit to the Beaucage model, Figure 1, shows that as the polymer concentration is increased, there is little change in the length scales or mass fractal of the semidilute polymer solution. This is further confirmed by the subplot, which shows the same data as Figure 1 but normalized for concentration. The only change observed is, at the lowest concentration, an increase in the high q regime that can be accounted for by the weak scattering being close to the incoherent background of this system. All concentrations could be fitted to a low-q fractal dimension of 2.1, a radius of gyration of the high q rod-like region of 74 Å, and a high-q fractal dimension of 1.1. For a semidilute polymer network, this length scale physically represents either the mesh size or the Kuhn length, whichever is shorter.

The radius of gyration of the rod-like subunit is reflected in Figure 1 by the q-value of the transition from a slope of −2.1 to −1.1 and can be converted into a length scale, which for this entangled polymer system corresponds to the length of the constituent rods, l_{rod}, forming the semiflexible entangled polymer solution. For this system, l_{rod} can be calculated through the radius of gyration of a thin rod, $l_{rod} = \sqrt{12R_s^{\,2}}$, and is calculated to be 25.6 nm, which is approximately twice the length of the previously measured persistence length of pectin.[21] Other measurements, not using small-angle scattering techniques, have reported the persistence length to be between 7 and 9 nm.[22,23] The only differences seen as the concentration of the polymer was increased were that the model more accurately fits to the measured scattering data. These data show that pectin in the solution state, in the absence of added salt, does not homogeneously fill space but instead has large regions that are polymer rich and other regions that are solvent rich. These can be thought of as tenuous dynamic aggregates that do not increase in density as the concentration is increased. If pectin homogeneously filled space, then the transition between the two power laws would move to a lower q when the concentration is increased. Indeed, dynamic light scattering measurements performed by the authors (see Supporting Information) and others[24] show a bimodal correlation function, even at concentrations far below the overlap concentration, that suggests tenuous aggregation, which has also been shown using other techniques.[25,26]

Rheological and Structural Evolution during Acid-Induced Gel Formation. After demethylesterification of this high-DM sample, GDL was introduced into solutions of the resulting blockwise low-DM polymer,[27] as described in the Experimental section, inducing a reduction in pH and concomitant gel formation. Figure 2, panel a shows the evolution of the rheological properties, measured at 1 Hz, after the introduction of GDL as its hydrolysis proceeds and the pH falls (see inset). Interestingly, and particularly evident in the 1% sample, is that before the significant increase (signaling macroscopic gel-formation), there is a slight decrease in the shear modulus. Figure 2, panel b shows the corresponding SAXS data, and with time, as the gelation proceeds, it can clearly be seen that the scattering at low q systematically increases in intensity and steepens in slope. This suggests that as the entangled pectin solution starts to associate and form local cross-links, polymer is drawn into more clustered regions that fill space less efficiently than the individual polymers and offers an explanation of the rheological data. In the early stages of the network formation, before these clusters are connected into a space spanning network, the clustered regions themselves draw polymer together and lower the effective concentration of the solution, temporarily reducing the storage modulus. As more clusters nucleate, grow, and connect, a space-spanning stress-bearing network is formed reflected in the growth of the storage modulus.

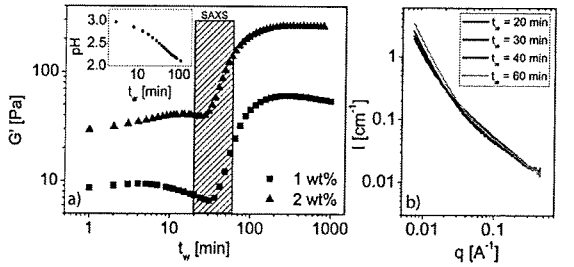

Figure 2. (a) Plot showing the evolution of the storage modulus, measured at 1 Hz, for 1 and 2 wt % acid gels and (b) time-resolved SAXS for the corresponding gels recorded at four different times after mixing (t_w).

Rheology and TEM of a Preformed Acid-Induced Gel. Once gels had reached the maximum strength, frequency-dependent prestress rheology experiments were performed to further mechanically characterize the system (Figure 3). Clear strain-stiffening is observed with the modulus of the systems increasing significantly with applied prestress. This behavior has indeed been reported previously in these acid-induced pectin gels where the data were shown to be consistent with the

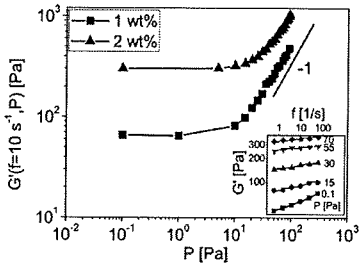

Figure 3. Plot showing the storage modulus as a function of applied prestress, P. The inset shows the frequency dependence of the storage modulus as the prestress is applied for 1 wt % data. The storage modulus shows a power law dependence of one, represented by the solid line guide, with increasing prestress.

DOI: 10.1021/acs.biomac.5b00870
Biomacromolecules 2015, 16, 3209−3216

Glassy Wormlike Chain model,[28] which also captured the reported microrheology of the system.[13] In general, stress-stiffening of networks has been shown to be a generic feature of systems in which the fundamental connecting elements deform according to a worm-like chain Hamiltonian.[29] It is worthwhile to note that, at least in the accessible prestress region, the increase of the differential shear modulus with prestress appears to increase linearly rather than with a power of 3/2 as predicted by the simple model.[30,31] This has been observed not only in acid-induced pectin gels, but also in calcium-assembled gels induced by controlled release of ions or the action of demethylesterifying enzymes, where the data were again well modeled.[32] While the rheological response then is highly suggestive of a network assembled from strands whose essential physics can be captured by those of a wormlike chain, several questions do remain including the distribution of sizes of such elements and the three-dimensional arrangement of the elastically active network chains in space. In an attempt to gather more information on the network architecture and provide some insight into these questions, a TEM tomography study was preformed as described in the Experimental section.

Figures 4 and 5 show TEM micrographs obtained from the final gelled system (a movie of the tomogram is available in the Supporting Information). It can be seen that the network has a somewhat clustered appearance with clusters of approximately a few hundred nanometers. Despite the significant difference in the strength of the fundamental bonding mediating the junction zones in these acid-induced networks and those in ionotropic pectin gels examined previously, the network architecture rendered here does not appear significantly different (a quantitative comparison is part of a larger study and will be published elsewhere). This indicates that perhaps the initial architecture of such systems at least is dominated by the nucleation and growth of nodes and less concerned with the strength of the connections (at least above several kT) that might dominate the dynamics and thermal stability to a much larger extent.

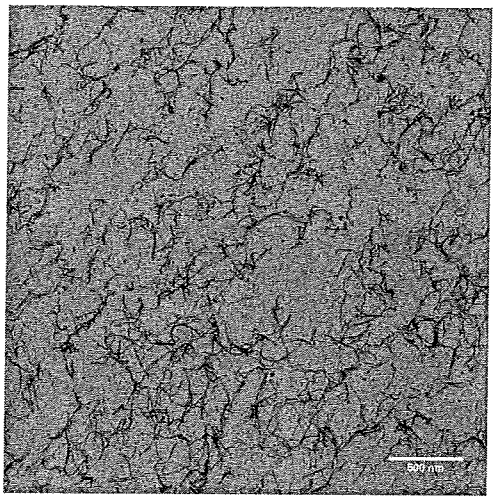

Figure 4. TEM micrograph of an acid-induced pectin gel prepared using GDL, as described in the text, showing the large scale network architecture.

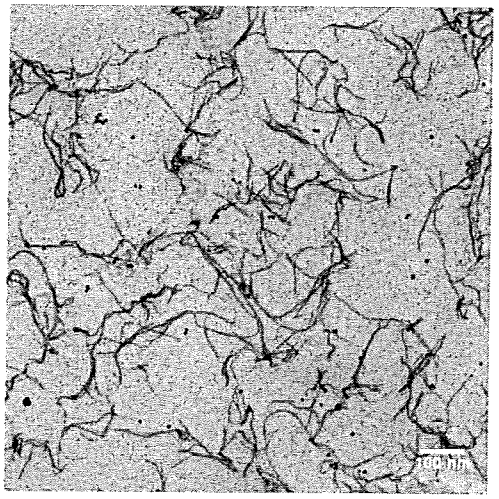

Figure 5. TEM micrograph of an acid-induced pectin gel prepared using GDL, as described in the text, showing the individual polymer entities forming the gel. The highly contrasted spots are colloidal gold particles added as fiducial markers to assist in the alignment of tomographic tilt series.

Structural Characterization of the Acid-Induced Gels as a Function of Temperature. In general, SAXS measurements carried out on the gelled samples (Figure 6) show a similar scattering profile to that obtained from pectin solutions (Figure 1), although with a drop in intensity in the high-q limit. This can be explained as an increase in the average radius of the scattering entities in the cross-linked system. To help further quantify the structural properties of this gelled system, a fit to a flexible cylinder form factor[33,34] with a fractal structure factor model[35] has been performed. The model is the same model as the worm-like chain model in the intermediate to high q regimes, although it includes a structure factor to take into account the low q scattering and was implemented using NCNR analysis macros for Igor, kindly made available by Steve Kline.[36] The model reveals that the network is primarily

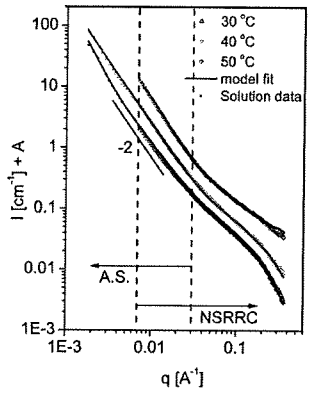

Figure 6. SAXS data for a 1 wt % acid-induced pectin gel formed with GDL, as described in the text, as the temperature is increased. Squares represent data taken at the Australian Synchrotron (AS) and open circles data taken at the NSRRC. It can be seen by 50 °C that the scattering from the melted gel resembles that taken for apple solution data at 30 °C. The solid lines represent a fit to a flexible cylinder form factor with fractal structure factor; refer to Table 1 for the fitting parameters. Data for 40 and 50 °C have been shifted for clarity, and 30 °C is plotted to an absolute intensity scale.

DOI: 10.1021/acs.biomac.5b00870
Biomacromolecules 2015, 16, 3209−3216

composed of dimeric entities with a Kuhn segment length of approximately 20 residues. This model was chosen since TEM micrographs showed significant bending in the polymeric entities forming the gel, and, as described, the rheological properties, in particular the observed strain-stiffening, can be captured by WLC network elements. It can indeed be seen (Figure 6) to provide an excellent fit to the scattering data obtained from these gels.

These hydrogen-bonded networks are well-known for their thermoreversibility and their melting at moderate temperatures (>50 °C), especially when compared to their calcium-formed cousins, and to investigate the structural changes occurring during such a process, preformed gels were heated in 10 °C increments while SAXS experiments were performed (Figure 6). At each step, the data were also fitted to the same model: at 40 °C, there is a significant drop in the size and Kuhn length of the scattering elements, as can be seen from Table 1. As the junction zones begin to dissolve at above 50 °C, the data show a profile very similar to that observed from the solution scattering of the individual polymers (for comparison, 1% solution data has been plotted in Figure 6 and shows almost an exact overlap with the melted gel, signaling its complete melting).

Table 1. Extracted Parameters When Fitting the Flexible Cylinder with Fractal Structure Factor Model Fitting. Errors Are Shown as ± One Standard Deviation

temperature	30 °C	40 °C
fractal dimension	2.6281 ± 0.0004	2.12 ± 0.01
contour length [Å]	2000	2000
Kuhn length [Å]	97.5 ± 0.3	93 ± 2
radius [Å]	7.056 ± 0.002	6.2 ± 0.2

Subsequently, further SAXS experiments were performed at the Australian Synchrotron SAXS beamline, an instrument capable of accessing smaller momentum transfer vectors. In overlapping q ranges, the data recorded on the different beamlines (NSRRC and AUS-SAXS) agreed well, shown in Figure 6. Here, to manipulate the key hydrogen-bonding strength, and also to make preliminary measurements to test the viability of performing small-angle neutron scattering on this system, we performed SAXS measurements on gels formed in pure D_2O, HDO, and H_2O (Figure 7a, b, and c, respectively). Lines in Figure 7 are drawn as a guide to the eye and show slopes between −3 and −4 in the low-q region indicating the presence of surface scattering form aggregates forming in the gel. These gels were formed at ambient temperatures using GDL to reduce the pH as described and were then heated while scattering data were aquired. Previous rheology measurements have shown that pectin acid gels are highly thermoreversible and can be melted and then cooled and reset with little hysteresis in the rheological properties.[10]

These SAXS measurements show that if the gels are held above the melting temperature for significant periods of time, there are structural changes that appear to be significant aggregation on the length scale of the order of hundreds to thousands of Angstrom, as seen by increases in the slopes shown in Figure 7. Further work here needs to be carried out to investigate these aggregations, as it is not clear if they are influenced by any chemical changes to the polymer. Chemical changes with heat are expected with pectin but at a pH close to neutral: at an acidic pH, as used here (see insert to Figure 2a), pectin is considered stable to moderate heat.[37] Previous experience with de-esterification methods and pectin chemistry suggests it is unlikely that significant chemical changes are occurring.[38,39] If chemical changes are not present, then clearly highly stable extensive aggregates could be formed at room temperature if they were not hindered by the formation of a network, and if the chains are allowed to interact uninhibited, then phase separation might be the ultimate fate of the system. The gelation process kinetically traps the system in a long-lived but out of equilibrium state. Indeed, a slow relaxation mode in pectin acid gels[13] and in other polysaccharide networks,[40−42] as found experimentally, can then be understood as arising from internal stresses created by the desire of the system to create longer junction zones. The method of de-esterification used to modify the polymer in this study created long runs of de-esterified regions with few shorter ones.[27] In effect, the lowest energy state of this pectin acid gel would be an aggregate that has completely phase separated into pure polymer and pure solvent regimes. Indeed, this brings to light the importance of knowledge about the esterification pattern along pectin chains, which is commonly overlooked and difficult to measure. Experiments on annealing these gels form future work.

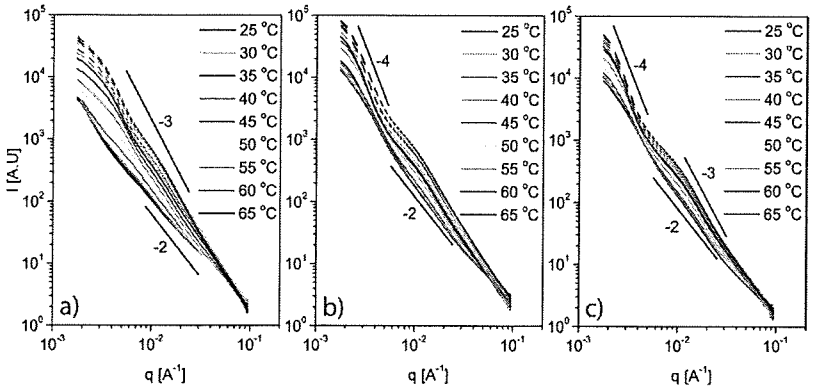

Figure 7. Plots showing SAXS data from acid-induced pectin gels formed in different solvents: (a) H_2O, (b) HDO, and (c) D_2O. Solid lines represent data recorded as the sample was heated and dashed lines the same sample as the temperature was reduced. The experiment was performed on a time scale of hours. It can be seen that gels formed in deuterated water are structurally different from those formed in water. All three samples appear to undergo aggregation upon heating, which is not reversible, as it is still present upon cooling. Solid lines are to guide the eye.

DOI: 10.1021/acs.biomac.5b00870
Biomacromolecules 2015, 16, 3209−3216

Also striking is the difference in fractal dimension, at 25 °C, between the gel formed in H_2O and the one formed in D_2O, which shows that the gel formed in D_2O is much more clustered. The cause of the difference needs further investigation, as little is known about the bonding in these networks, and it is unclear if the difference is due to solvent polymer interaction, stronger binding due to the solvent playing a part in the hydrogen bonding, or the conformation of the pectin chain changing. Nevertheless, this highlights the need to be mindful of changes induced when substituting D_2O in systems with significant hydrogen bonding.

CONCLUSION

SAXS measurements revealed the structure of acid-induced pectin gels to be clustered networks composed of flexible, cylindrical elements with an average radii of 7 Å and Kuhn lengths of 97.5 Å at 30 °C. The flexible rod-like nature of the network was indeed clearly visible using TEM, and despite the similarities in the overall network architecture, the flexibility of the fundamental network elements is in contrast to the more rod-like junctions found in pectin calcium gels. Measurements on networks formed in deuterium oxide show substantial differences in the network clustering bringing further to light the importance of hydrogen bond formation in these networks and highlighting that care must be taken when using deuterated solvents if hydrogen bonding is important.

ASSOCIATED CONTENT

Supporting Information

The Supporting Information is available free of charge on the ACS Publications website at DOI: 10.1021/acs.biomac.5b00870.

Dynamic light scattering data of a dilute blocky pectin solution (PDF)

TEM tomography data corresponding to an area in the sample of 1.87 × 1.73 μm^2 (AVI)

AUTHOR INFORMATION

Corresponding Author

*E-mail: m.williams@massey.ac.nz.

Present Address

$^{\nabla}$SP Food and Bioscience, PO Box 5401, 402 29 Gothenburg, Sweden

Notes

The authors declare no competing financial interest.

ACKNOWLEDGMENTS

The authors thank Romaric Vincent for interesting discussions, The Royal Society of New Zealand for the Taiwan exchange funding, the Australian synchrotron for proposal 7612, and the New Zealand Synchrotron group for travel funding.

REFERENCES

(1) Willats, W. G. T.; McCartney, L.; Mackie, W.; Knox, J. P. *Plant Cell Walls*; Carpita, N. C., Campbell, M., Tierney, M., Eds.; Springer: The Netherlands, 2001; pp 9–27.

(2) Thakur, B. R.; Singh, R. K.; Handa, A. K.; Rao, M. A. *Crit. Rev. Food Sci. Nutr.* **1997**, *37*, 47–73.

(3) Willats, W. G. T.; Knox, J. P.; Mikkelsen, J. D. *Trends Food Sci. Technol.* **2006**, *17*, 97–104.

(4) Peaucelle, A.; Braybrook, S.; Höfte, H. *Front. Plant Sci.* **2012**, *3*, 121.

(5) Liu, L.; Fishman, M. L.; Kost, J.; Hicks, K. B. *Biomaterials* **2003**, *24*, 3333–3343.

(6) Vincken, J.-P.; Schols, H. A.; Oomen, R. J. F. J.; McCann, M. C.; Ulvskov, P.; Voragen, A. G. J.; Visser, R. G. F. *Plant Physiol.* **2003**, *132*, 1781–1789.

(7) Powell, D. A.; Morris, E. R.; Gidley, M. J.; Rees, D. A. *J. Mol. Biol.* **1982**, *155*, 517–531.

(8) Rees, D. A. *Advances in Carbohydrate Chemistry and Biochemistry*; Academic Press: New York, 1969; Vol. *24*; pp 267–332.

(9) Rubinstein, M.; Dobrynin, A. V. *Curr. Opin. Colloid Interface Sci.* **1999**, *4*, 83–87.

(10) Gilsenan, P. M.; Richardson, R. K.; Morris, E. R. *Carbohydr. Polym.* **2000**, *41*, 339–349.

(11) Stang Holst, P.; Kjøniksen, A.-L.; Bu, H.; Sande, S. A.; Nyström, B. *Polym. Bull.* **2006**, *56*, 239–246.

(12) Ström, A.; Schuster, E.; Goh, S. M. *Carbohydr. Polym.* **2014**, *113*, 336–343.

(13) Vincent, R. R. R.; Mansel, B. W.; Kramer, A.; Kroy, K.; Williams, M. A. K. *New J. Phys.* **2013**, *15*, 035002.

(14) Liu, D.-G.; Chang, C.-H.; Liu, C.-Y.; Chang, S.-H.; Juang, J.-M.; Song, Y.-F.; Yu, K.-L.; Liao, K.-F.; Hwang, C.-S.; Fung, H.-S.; et al. *J. Synchrotron Radiat.* **2009**, *16*, 97–104.

(15) Kirby, N. M.; Mudie, S. T.; Hawley, A. M.; Cookson, D. J.; Mertens, H. D. T.; Cowieson, N.; Samardzic-Boban, V. *J. Appl. Crystallogr.* **2013**, *46*, 1670–1680.

(16) Zemb, T.; Lindner, P. *Neutrons, X-rays, and Light: Scattering Methods Applied to Soft Condensed Matter*; Elsevier: North Holland, The Netherlands, 2002.

(17) Li, Y.-C.; Chen, K.-B.; Chen, H.-L.; Hsu, C.-S.; Tsao, C.-S.; Chen, J.-H.; Chen, S.-A. *Langmuir* **2006**, *22*, 11009–11015.

(18) Beaucage, G. *J. Appl. Crystallogr.* **1996**, *29*, 134–146.

(19) Beaucage, G. *J. Appl. Crystallogr.* **1995**, *28*, 717–728.

(20) Hammouda, B. *J. Appl. Crystallogr.* **2010**, *43*, 1474–1478.

(21) Cros, S.; Garnier, C.; Axelos, M. A. V.; Imberty, A.; Pérez, S. *Biopolymers* **1996**, *39*, 339–351.

(22) Axelos, M. A.; Thibault, J. F. *Int. J. Biol. Macromol.* **1991**, *13*, 77–82.

(23) Malovikova, A.; Rinaudo, M.; Milas, M. *Carbohydr. Polym.* **1993**, *22*, 87–92.

(24) Lima, A. M. F.; Soldi, V.; Borsali, R. *J. Braz. Chem. Soc.* **2009**, *20*, 1705–1714.

(25) Davis, M. A. F.; Gidley, M. J.; Morris, E. R.; Powell, D. A.; Rees, D. A. *Int. J. Biol. Macromol.* **1980**, *2*, 330–332.

(26) Sorochan, V. D.; Dzizenko, A. K.; Bodin, N. S.; Ovodov, Y. S. *Carbohydr. Res.* **1971**, *20*, 243–249.

(27) Williams, M. A. K.; Cucheval, A.; Nasseri, A. T.; Ralet, M.-C. *Biomacromolecules* **2010**, *11*, 1667–1675.

(28) Kroy, K.; Glaser, J. *New J. Phys.* **2007**, *9*, 416.

(29) Storm, C.; Pastore, J. J.; MacKintosh, F. C.; Lubensky, T. C.; Janmey, P. A. *Nature* **2005**, *435*, 191–194.

(30) Blundell, J. R.; Terentjev, E. M. *Macromolecules* **2009**, *42*, 5388–5394.

(31) Carrillo, J.-M. Y.; MacKintosh, F. C.; Dobrynin, A. V. *Macromolecules* **2013**, *46*, 3679–3692.

(32) Schuster, E.; Lundin, L.; Williams, M. A. K. *Macromolecules* **2012**, *45*, 4863–4869.

(33) Pedersen, J. S.; Schurtenberger, P. *Macromolecules* **1996**, *29*, 7602–7612.

(34) Chen, W.-R.; Butler, P. D.; Magid, L. J. *Langmuir* **2006**, *22*, 6539–6548.

(35) Teixeira, J. *J. Appl. Crystallogr.* **1988**, *21*, 781–785.

(36) Kline, S. R. *J. Appl. Crystallogr.* **2006**, *39*, 895–900.

(37) Sajjaanantakul, T.; van Buren, J. P.; Downing, D. L. *J. Food Sci.* **1989**, *54*, 1272–1277.

(38) Williams, M. A. K.; Foster, T. J.; Schols, H. A. *J. Agric. Food Chem.* **2003**, *51*, 1777–1781.

(39) Ström, A.; Williams, M. A. K. *Carbohydr. Res.* **2004**, *339*, 1711–1716.

(40) Larobina, D.; Cipelletti, L. *Soft Matter* **2013**, *9*, 10005–10015.

DOI: 10.1021/acs.biomac.5b00870
Biomacromolecules 2015, 16, 3209–3216

(41) Secchi, E.; Roversi, T.; Buzzaccaro, S.; Piazza, L.; Piazza, R. *Soft Matter* **2013**, *9*, 3931−3944.
(42) Secchi, E.; Munarin, F.; Alaimo, M. D.; Bosisio, S.; Buzzaccaro, S.; Ciccarella, G.; Vergaro, V.; Petrini, P.; Piazza, R. *J. Phys.: Condens. Matter* **2014**, *26*, 464106.

DOI: 10.1021/acs.biomac.5b00870
Biomacromolecules 2015, 16, 3209−3216